A computational study of the mechanism of palladium insertion into alkynyl and aryl carbon–fluorine bonds †

Markus Jakt, Linus Johannissen, Henry S. Rzepa,* David A. Widdowson and René Wilhelm

Department of Chemistry, Imperial College of Science, Technology and Medicine, London, UK SW7 2AY

Received (in Cambridge, UK) 25th September 2001, Accepted 17th December 2001
First published as an Advance Article on the web 25th January 2002

An *ab initio* molecular orbital study using both gas-phase and B3LYP/DZVP-COSMO solvation models of the mechanism of palladium insertion into alkyne and aryl carbon–halogen bonds suggests that the mechanism of palladium insertion into alkyne species can proceed *via* a concerted oxidative addition across the carbon–halogen bond. A stepwise mechanism *via* a σ-complex is favoured when a nitro group is introduced onto the alkyne. The palladium insertion into variously substituted aryl fluorides was again found to proceed *via* a single-step concerted mechanism, and although a σ-complex can be located when 2,4-dinitro and 2-nitro substitution is present, the energy of this stepwise route is very similar to the concerted pathway and no clear decision on the pathway can be made. No intermediate σ-complex could be located for η^6-tricarbonylchromium-complexed fluorobenzene, and only a concerted pathway was identified.

Introduction

Palladium catalysed cross-coupling reactions have found an important place in modern synthetic protocols (Scheme 1).[1] The

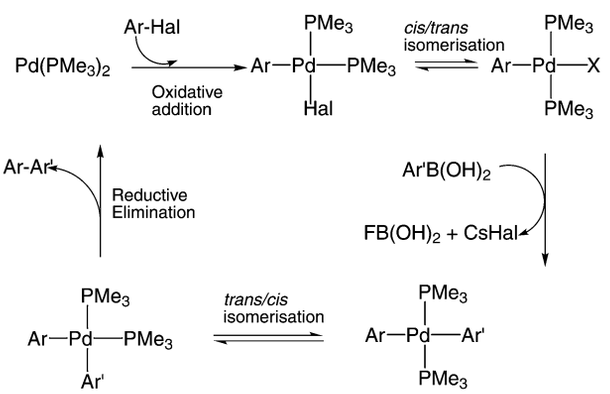

Scheme 1

first step of these reactions is the insertion of a palladium(0) species into a carbon–halogen or in special cases, a carbon–oxygen bond.[1] Although aryl iodides, bromides and triflates are most commonly used, recently aryl chlorides, hitherto regarded as inert to palladium catalysed cross-coupling reactions, have been shown to be effective participants provided there is an electron-withdrawing group on the aryl ring[2] (including the η^6-tricarbonylchromium(0) group)[3] and/or a basic phosphine ligand[4–8] on the palladium. In contrast, fluoroarenes in palladium cross-coupling reactions were not described in the literature prior to our work on fluoroarenechromium(0) complexes.[9,10] The C–F bond is the strongest of the C–halide bonds,[11] cleavage of which is only described for multifluorinated compounds,[12] in oxidative addition of nickel[13,14] or by nucleophilic aromatic substitution of electron deficient fluoroarenes[11] and fluoroarenechromium(0) complexes.[15,16] Although our earlier work with chromium complexes[9,10] and fluoronitroarenes,[17] revealed a palladium catalysed cross-coupling process analogous to Suzuki and Stille reactions, the exact mechanism remained unproven and this prompted us to carry out calculations to further explore the possible mechanism(s) of the reaction, the results of which we present here.

Computational procedure

Molecular structures were optimised using either GAMESS[18] or Gaussian 98,[19] the two programs giving identical results at the RHF closed shell level. RB3LYP correlated calculations were done exclusively using Gaussian98. The 3-21G* basis was used for pathfinding calculations, which was then extended to an all electron DZVP[20] externally introduced basis set for all atoms. In order to determine the nature of the structures derived from these calculations, calculation of the second derivative matrix was used to verify transition states as having only one imaginary normal mode and equilibrium geometries states as having none. IRC (intrinsic reaction coordinate) calculations were run starting from transition state geometries in both directions, which verified that either **1** or **7** and **3** linked the located transition state. Solvation calculations were carried out with Gaussian 98 using the COSMO model [keyword: "SCRF = (CPCM)"] with a permittivity of 78.4 for water as solvent. Geometry optimisation with this keyword set proved poorly convergent for some systems, and the LOOSE keyword was then employed. In some cases, even this relaxation did not facilitate optimisation, as noted in the text. Transition state normal modes and IRC paths were animated by viewing the Gaussian log files using JMol. Coordinates and normal mode animations are available as supplementary data. †

Results and discussion

1 Ethynyl systems

We initially used as models the computationally faster alkynyl systems (Table 1) to simplify our exploration of these potential surfaces. This methodology had proved expedient in our earlier studies of the related iodine(I)/(III) insertion/eliminations across a C–F bond.[21] The key stationary points for the insertion of $Pd(PR'_3)_2$ (R′ = H, Me) into alkynyl halides are indicated in

† Electronic supplementary information (ESI) available: full coordinates for all geometries and normal mode animations. See http://www.rsc.org/suppdata/p2/b1/b108727b/

 DOI: 10.1039/b108727b

Table 1 Relative energies/kcal mol^{-1} (total energies given for **1** in hartree) and first order stationary points [transition wavenumber/cm^{-1}] for insertion of $Pd(PH_3)_2$ into substituted haloalkynes

R–CC–Hal		RHF/3-21G*		RHF/DZVP		RB3LYP/DZVP	
R	Hal	Stationary point	*E*/Δ*E*	Stationary point	*E*/Δ*E*	Stationary point	*E*/Δ*E*
H	F	**1**	−5771.4516 (0)	**1**	−5797.7672 (0)/−6032.0060[a]	**1**	−5802.5714 (0) {6038.5230 (0)}[a]
		2	32.9/[486.4]	**2**	56.9/[541.0] {(48.2)}[a]	**2**	27.8 {21.1}[a]
		3	−17.2	**3**	−3.8	**3**	−7.5
H	Cl	**1**	−6129.9664 (0)	**1**	−6157.7692 (0)	**1**	−6162.8895 (0)
		2	20.5 [382.5]	**2**	37.21 [465.3]	**2**	14.07 [195.8]
		3	−28.8	**3**	−9.0	**3**	−16.7
H	Br	**1**	−8232.8362 (0)	**1**	−8270.2062 (0)	**1**	−8276.4155 (0)
		2	−6.7 [260.2]	**2**	27.80 [346.3]	**2**	−7.33 [109.4]
		3	−35.2	**3**	−15.1	**3**	−21.8
H	I	**1**	−12560.4793 (0)	**1**	−12615.4775 (0)	**1**	−12622.5911 (0)
		2	—	**2**	19.0 [265.5]	**2**	2.75 [62.7]
		3	−30.6	**3**	−16.0	**3**	−22.5
NO_2	F	**1**	−5973.7081 (0)	**1**	−6001.2184 (0)	**1**	−6007.0821 (0) {−6007.0796 (0)}[b]
		4	—	**4**	3.77 [153.4]	**4**	—
		5	−24.4	**5**	−8.4	**5**	−28.2
		6	—	**6**	—	**6**	{1.5}[b]
		7	—	**7**	19.1	**7**	3.9 {−10.8}[b]
		8	—	**8**	—	**8**	{−6.2}[b]
		2	10.7 [375.2]	**2**	33.82 [478.8]	**2**	10.10 [328.3]
		3	−29.5	**3**	−6.3	**3**	−16.4 {−30.2}[b]
CN	F	**1**	−5862.6693 (0)	**1**	−5889.4958 (0)	**1**	−5894.8206 (0)
		5	−13.6	**5**	−1.38	**5**	−21.2
		2	20.02 [405.3]	**2**	42.80 [498.8]	**2**	15.69 [376.3]
		3	−25.0	**3**	−4.4	**3**	−14.8
NH_2	F	**1**	−5826.1742 (0)	**1**	−5852.7885 (0)	**1**	−5857.9280 (0)
		2	31.4 [442.6]	**2**	52.5 (488.12 cm^{-1})	**2**	26.0 [286.2]

[a] Results for R′ = Me (PMe_3). [b] COSMO Solvation model with geometry optimisation, using LOOSE convergence criteria.

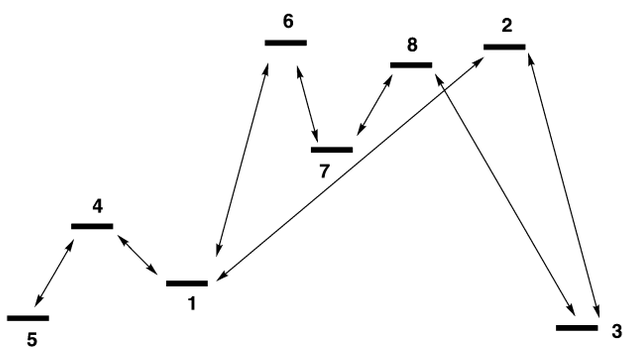

Scheme 2

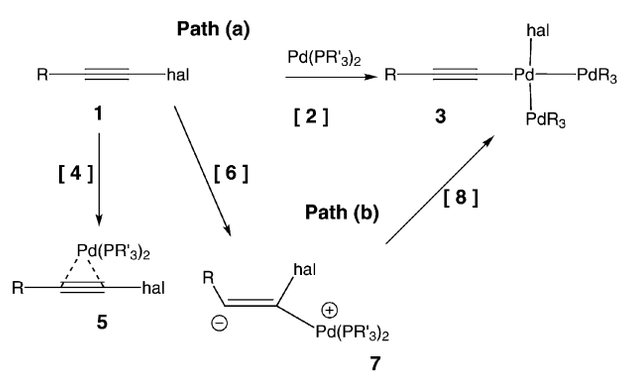

Scheme 3

Scheme 2, with structures in Scheme 3. Three possible reaction outcomes were investigated from the reactants **1**. Concerted oxidative addition of the Pd across the C–halide bond could proceed *via* a transition state **2** to give the Pd(II) species **3**. An alternative stepwise route involves nucleophilic addition by Pd(0) to give a dipolar intermediate **7** bounded by the transition state **6** for C–Pd formation and **8** for C–halogen elimination, followed by collapse to **3**. For alkynyl systems, a π-complex **5** can also be formed *via* transition state **4**.

Dependence on basis set and level of theory. The calculated geometries at three levels of theory are collected in Fig. 1, and those specifically for nitrofluoroethyne in Fig. 2. Energies are summarised in Table 1. All initial approximations to stationary points were calculated at the relatively fast RHF/3-21G* basis level, but we realised that at this level, not all of the stationary points existing within a shallow potential could always be located. More reliable results were sought by improving the basis set to the all-electron double zeta valence polarisation set (DZVP). This has the effect of increasing calculated barriers compared with the 3-21G* level by about 20–23 kcal mol^{-1}. Further correction for correlation energy, *via* the RB3LYP procedure, reduces the barriers by a similar amount. We also established that the approximation of using PH_3 as a model ligand instead of the ligand PMe_3 used in practice overestimates the computed barriers by about 8 (RHF) or 6 kcal mol^{-1} (RB3LYP). These various corrections result in a predicted gas-phase barrier to reaction of about 21 kcal mol^{-1} for insertion across fluoroethyne, corresponding to a relatively facile thermal reaction.[1] The alkynyl reactions are predicted to be exothermic at all levels of theory (Table 1).

Substituent effects on the ethyne series. Our initial efforts concentrated on establishing the trend across the series Hal = F–I *via* the alkyne series and showed that the activation energy for concerted oxidative addition *via* transition state **2** decreases, whilst the exothermicity of reaction increases along the series Hal = F, Cl, Br and I. Insertions across Cl, Br and I are all well established.[1] The barrier for Hal = I was very small at the larger basis set level, and no transition state could be located at the smaller 3-21G* level. We also demonstrated that an electron-withdrawing group R on the other terminus of the ethyne significantly decreases the barrier and increases the exothermicity

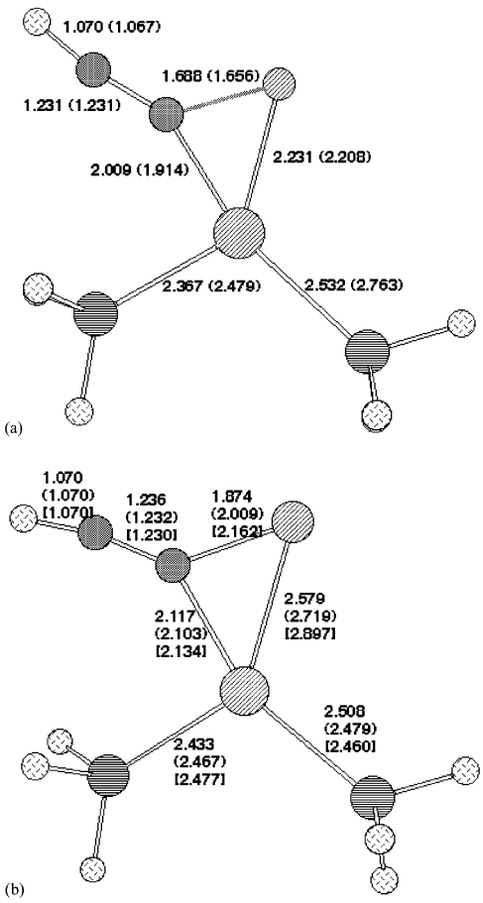

Fig. 1 Calculated geometries for (a) transition state **2** for insertion of $Pd(PH_3)_2$ into **1**, R = H, Hal = F. Bond lengths (Å) for RB3LYP//DZVP (RHF//DZVP) and (b) into R–CC–Hal, R = H, Hal = Cl, Br and I. Bond lengths (Å) for RB3LYP//DZVP, Hal = Cl (Hal = Br) [Hal = I]. Full coordinates for all geometries are available as supplementary data.†

of the reaction, whereas the electron donating group R = NH_2 has an insignificant effect.

The other major effect along the series Hal = F, Cl, Br, I is that the geometry of the transition states tends towards tetrahedrality. For chlorine the effect is small, but is more apparent for bromine and chlorine.† In the RB3LYP DZVP transition state for Hal = I, the Pd–P bond of the phosphine *trans* to the halide is only slightly longer than that of the *cis* phosphine. As the halide becomes more electronegative, both Pd–P bonds decrease and become less equal in length. Eventually, the longer Pd–P bond corresponds to the *cis* phosphine and is greatest for Hal = F where the *trans* Pd–P bond is 2.532 *vs.* 2.367 Å for the *cis* Pd–P bond. This can be explained by an increasing degree of pπ-bonding interactions between the *trans* phosphine and the alkyne, which also explains the planar geometry for the Hal = F, Cl transition states compared to the twisted geometry for Hal = Br, I.

Addition to fluoronitroethyne (1, R = NO_2, Hal = F). We next focused on **1**, R = NO_2, Hal = F, for initial exploration of the mechanism of addition across C–F bonds activated by the presence of an electron-withdrawing group (Fig. 2, Table 1). The π-complex formed by direct coordination of the metal to the ethyne (**5**) is predicted to be more stable than the product **3** of C–F addition (Table 1). We note this system is analogous to the reported isolation of a η^2-nickel–aryl π-complex.[14] The stability of **5** is explained by looking at the metal–alkyne synergic bonding, which is composed of electron donation of the metal d-orbitals into the empty π* orbital, and back-donation from the π-orbital of the C=C double bond. In this case, however, the C=C π-orbital in the same plane as the nitro group is very electron deficient; the alkyne therefore orientates itself so that the back-bonding occurs from the π-orbital perpendicular to the nitro group. These π-complexes are probably not active intermediates in the palladium insertion reaction, as was proposed for the oxidative addition of nickel to an octafluoronaphthalene C–F bond.[14] Instead, once a π-complex is formed, we believe it must re-dissociate *via* transition state **4** if the palladium insertion reaction is to proceed.

Whereas IRC (intrinsic reaction coordinate) calculations from the transition state **2**, R = H, CN; Hal = F, led directly to **1** or **3**, that for R = NO_2 resulted in the location of an intermediate **7**. For this particular case, therefore, the stationary point numbered **2** for a gas-phase pathway corresponds to either **6** or **8** on an ionic pathway. This change directly relates to the two possible mechanistic pathways we noted for oxidative addition across a C–halogen bond in Scheme 3. Path (a) corresponds to a concerted (non-ionic) oxidative addition across the carbon–halogen bond involving transition state **2** whereas path (b) is a stepwise (ionic) reaction involving the formation of an intermediate zwitterionic complex **7** bounded by transition states **6** and **8**. The complex **7** is expected to be particularly stabilised by the presence of highly electron-withdrawing substituents.

Since significant stabilisation of the zwitterion by solvent would be expected, we applied the RB3LYP//DZVP-COSMO model for evaluating the free energy of solvation, including the free energy corrections for creating the appropriate solvent cavity. Water as solvent was chosen to simulate the maximum reasonable solvation effect. We found that the energies of the gas-phase geometry **2** and **7** are lowered by 11.1 and 9.5 kcal mol^{-1} respectively when a single point calculation is performed. When the geometry is re-optimised with inclusion of the solvation model, the energy of **7** decreases by a further 3.5 kcal mol^{-1}, resulting in a species which is significantly more stable than the reactants. The magnitude of the solvation energy is quite modest for a zwitterionic species; that for the glycine zwitterion for example is 41 kcal mol^{-1} at the same level of theory (with additional solvation having its origin in specific hydrogen bonding with solvent). The overall product **3** is similarly stabilised by solvation, whereas the energy of the reactants **1** is essentially unaffected (Table 1).

The geometry of **7** (R = NO_2) (Fig. 2) reveals that the π-orbitals of the nitro group are coplanar with the carbanionic lone pair and this results in stabilisation through π-interaction. The carbanionic lone pair is also anti-periplanar to the C–F bond, indicating considerable interaction between it and the C–F π-antibonding orbital. The geometry at the Pd centre reveals the Pd–C bond to be axial, along with one Pd–P ligand, the other being equatorial. The C–F bond distance of 1.416 Å is elongated compared with normal vinyl fluorides (*ca.* 1.28–1.3 Å), consistent with the anti-periplanar interaction, as noted above, weakening this bond as a preliminary to either complete dissociation to form fluoride anion, or of migration to the Pd centre without complete dissociation.

The two transition states (in a solvation model) leading out of the intermediate, **6** corresponding to formation/cleavage of the C–Pd bond and **8** to formation/cleavage of the C–F bond, correspond to barriers of 12.2 and 4.5 kcal mol^{-1} respectively. Thus with a solvent model applied, transition state **6** replaces the concerted gas-phase transition state **2**, and the overall barrier to reaction from **1** is now only 1.5 kcal mol^{-1} and hence the kinetics are likely to be controlled by entropic rather than enthalpic terms.

2 Palladium insertion into substituted aryl fluorides

The potential surface for Pd insertion into aryl halides is analogous to that shown in Schemes 2 and 3, with the exception that **5** was not located. The geometry for a series of substituted derivatives is shown in Fig. 3 and the energies are given in

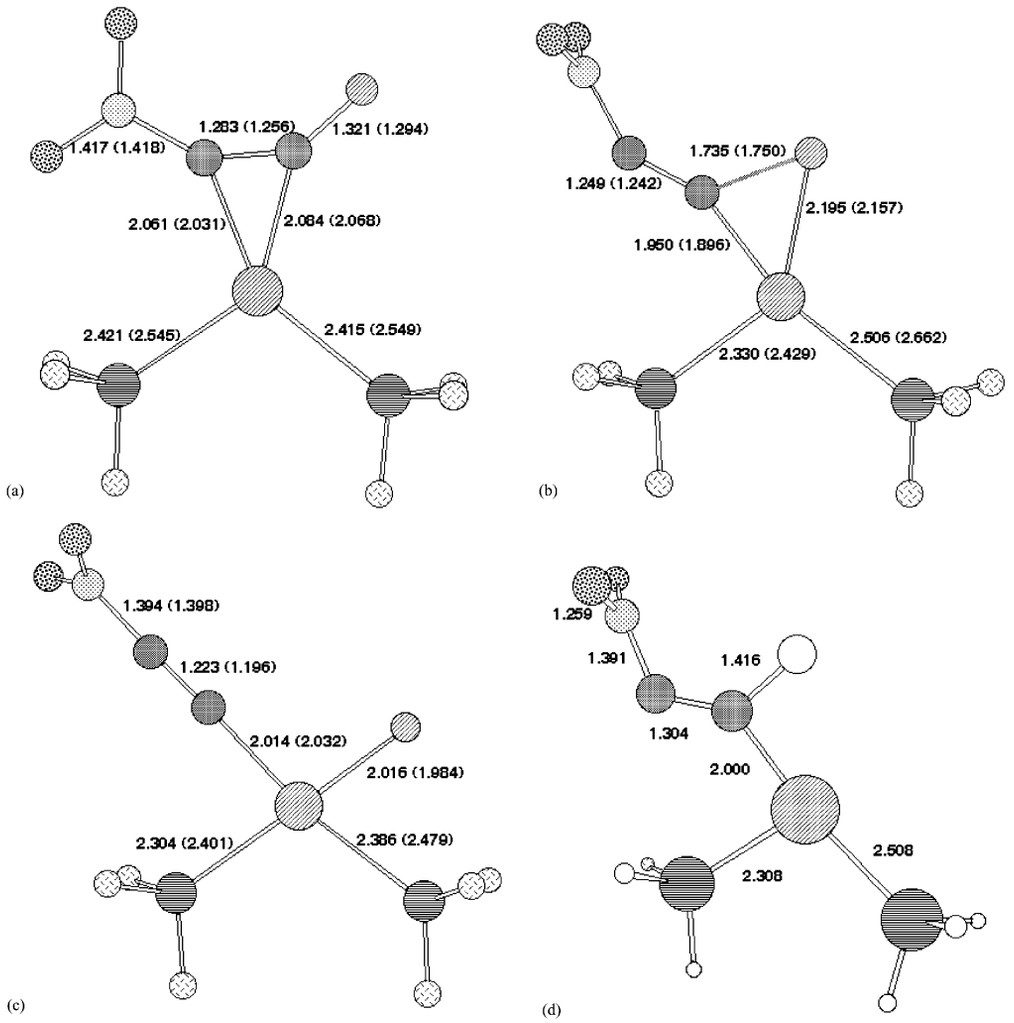

Fig. 2 Calculated geometries for stationary point (a) **5**, (b) **2**, (c) **3** and (d) **7** on the potential surface for insertion of $Pd(PH_3)_2$ into **1**, R = O_2N, Hal = F. Bond lengths (Å) for B3LYP//DZVP (RHF//DZVP). The geometry of **7** was obtained using the COSMO solvation model.

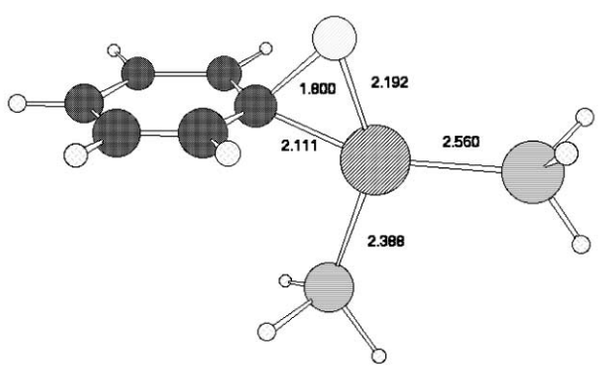

Fig. 3 Calculated bond lengths (Å/B3LYZ/DZVP) for transition state **2** for fluorobenzene.

Table 2. The RB3LYP/DZVP level was used exclusively for studying these aryl systems. The insertion barriers are similar to those reported for Pt(O) insertions are at a similar level of theory.[22] The effect of a single electron-withdrawing group on the activation energy is less for the aryl than for the ethyne species. The calculated B3LYP//DZVP activation energy for fluoroethyne drops by 17.7 kcal mol^{-1} when a nitro substituent is introduced, whereas the aryl analogue is reduced by 5.7 (4-NO_2), 13.1 (2-NO_2), and an approximately additive 19.4 (2,4-di-NO_2) kcal mol^{-1}. The most significant effect here is the apparently anomalous result for R = 2-NO_2, which is attributable to interaction between the nitro group and the Pd centre

Table 2 Relative energies/kcal mol^{-1} (total energies for **1** in hartree) and transition states **2** [transition wavenumber/cm^{-1}] for insertion of $Pd(PH_3)_2$ into aryl fluorides

R–aryl–F R		RB3LYP/DZVP E/E_h, gas phase	RB3LYP/DZVP E/E_h, COSMO
H	**1**	−5957.5279 (0)	−5957.5331
	2	41.2 [360.7]	−5957.4691 (40.2)
$Cr(CO)_3$	**1**	−7341.9547 (0)	−7341.9592
	7	[a]	Optimises to **1** or **3**[a]
	2	40.0 [322.4]	37.8
	3	13.4	[4.7][a]
2-NO_2	**1**	−6162.0548 (0)	−6162.0629
	7	[a]	− [22.7][a]
	2	28.1 [296.4]	−6162.0159 (29.4)
4-NO_2	**1**	−6162.0661 (0)	−6162.0738
	2	35.5 [336.2]	−6162.0178 (35.1)
2,4-NO_2	**1**	−6366.5868 (0)	−6366.5892
	7	[a]	−[7.4][a]
	2	21.8 [278.0][a]	18.0
	3	[5.2][a]	[−4.1][a]
2-CN	**1**	−6049.7744 (0)	−6049.7801
	7	[a]	Optimises to **1** or **3**[a]
	2	35.5 [341.5]	−6049.7219 (36.5)
4-CN	**1**	−6049.7778 (0)	−6049.7861
	2	37.02 [343.9]	−6049.7258 (37.8)

[a] Geometry optimised (to LOOSE tolerances) with COSMO model. Geometry not locatable with gas-phase model.

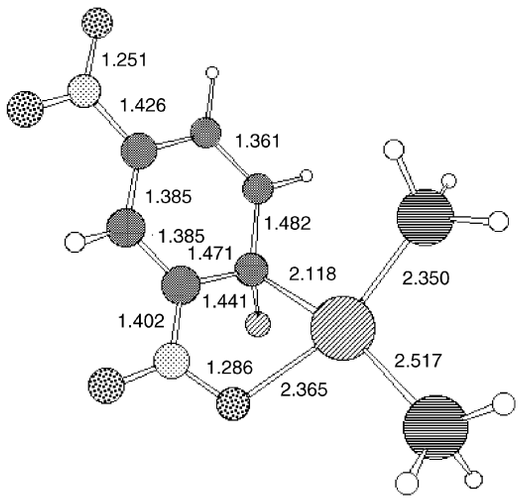

Fig. 4 Calculated bond lengths (Å/B3LYP//DZVP/COSMO) for the complex **7** originating from 2,4-dinitrofluorobenzene.

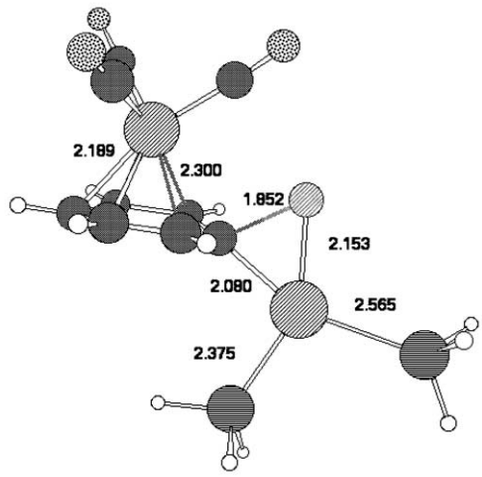

Fig. 5 Calculated bond lengths (Å/B3LYP//DZVP) for the transition state **2** originating from η^6-chromium tricarbonyl fluorobenzene.

(*cf.* Fig. 4). The linear geometry of a CN substituent does not allow such an interaction, and here the barrier lowering is very similar for R = 4-CN (4.2) and R = 2-CN (5.7). We note the similarity of this result to a report of *ab initio* calculations on aromatic substitution of differently substituted aryl halides,[23] which revealed that such reactions are predicted to proceed *via* a single-step mechanism when no electron-withdrawing group is present, albeit with very high energy barriers. The introduction of electron-withdrawing nitro groups lowered the barrier, but the presence of two nitro groups resulted in a multi-step reaction.

The COSMO solvation model was used to probe whether the stepwise mechanism [path (b), Scheme 3] is energetically viable for the Pd insertion reaction. Calculations at the gas-phase geometry revealed quite small solvation-induced changes in the barrier, ranging from -3.8 kcal mol^{-1} for 2,4-dinitro, to about $+1$ kcal mol^{-1} for 2- or 4-CN, which implied that an S_NAr mechanism [path (b)] is not viable. However, re-optimisation of the geometry with solvation applied did result in the location of **7** for 2-NO_2 and 2,4-NO_2 (Table 2). The geometry of this latter species (Fig. 4) is noteworthy for the relatively long C–F bond, suggesting a very low barrier for elimination of fluoride anion.

Starting from this optimised geometry, but replacing nitro by cyano and again re-optimising with this substituent led only to the reactant **1**, a repeat of the behaviour found in the alkyne series. This again confirms that pathway (b) is only possible with nitro ring substitution. Location of the two transition states **6** and **8** for this system proved problematic, since the Gaussian COSMO geometry optimisation was found to be unstable and poorly convergent for all controlling parameters investigated. Assuming similar barriers of about 12 and 5 kcal mol^{-1} out of **7** as were found for the alkyne system would result in an energy for **6** very similar to the barrier for **2**. We conclude that for the nitroaryl series, the mechanistic pathway (b) would only occur in highly polar solvents, and that it may not constitute a significantly lower reaction pathway than mode (a).

Palladium insertion into η^6-$Cr(CO)_3$-fluorobenzene. Our final analysis was of reaction of the η^6-tricarbonyl chromium fluorobenzene species, a reaction that we have recently reported[9,10] occurs in good yields. Houk and co-workers have similarly reported[24] that the $Cr(CO)_3$ ligand significantly reduces the barrier towards nucleophilic (anionic) attack at benzene. Our calculated geometry of the transition state **2** reveals the C–F bond to be eclipsed with respect to one Cr–CO group (Fig. 5). After the transition state is passed rotation of the $Cr(CO)_3$ group occurs to remove unfavourable steric interactions between the Pd substituent and the $Cr(CO)_3$. Unlike the alkynyl series, the reaction is calculated to be endothermic in the gas phase (Table 2). The difference in the reaction energy between R = $Cr(CO)_3$ and R = 2,4-NO_2 appears to mostly originate in the Pd–O stabilising interaction in the latter.

The calculated gas-phase activation barrier of 40.0 kcal mol^{-1} is higher than the activation barrier for insertion into to both 2,4-dinitrofluorobenzene and 4-nitrofluorobenzene. By analogy with the alkynyl series, we anticipate this barrier would be reduced by about 6 kcal mol^{-1}, if PMe_3 ligands replaced PH_3, a barrier which is still too high for the facile thermal reaction for this substituent that we observe experimentally. This barrier is reduced by only about 2 kcal mol^{-1} when the COSMO model is applied to the gas-phase geometry. Geometry optimisation using as a starting point the key parameters obtained for **7**, R = 2,4-NO_2, does not result in the zwitterionic species **7** but rather in reactant **1**. Attempts to locate **7**, R = $Cr(CO)_3$, starting from either an eclipsed or a staggered orientation of the $Cr(CO)_3$ group also gave this result. We note however that a related species has indeed been isolated from anionic (rather than zwitterionic) addition to $Cr(CO)_3$-benzene.[25] This species also has an eclipsing interaction between one Cr–CO bond and the C–H bond at which nucleophilic addition has occurred.

Our failure to locate **7**, R = $Cr(CO)_3$, with Pd as nucleophile may relate at least in part to steric factors. Thus, the Pd group would have to approach from the aryl face opposite to that coordinated by Cr, and this in turn must force the F atom and its lone pairs into conflict with the eclipsing carbonyl group and its π-cloud. A secondary effect is that the η^6 coordination of the Cr to the arene ring is significantly reduced (approximately η^3, Fig. 5), and this is apparently not compensated by the forming C–Pd bond. This problem is lessened for the 2-nitro or 2,4-dinitrophenyl systems by additional stabilisation of the Pd *via* O $\cdots$ Pd coordination (Fig. 4). Finally we note here that the COSMO model stabilises the product compared to reactant for both R = $Cr(CO)_3$ and R = 2,4-NO_2, and hence solvation may be the prime thermodynamic driving force for these reactions.

Conclusions

Our study of the alkynyl series has revealed that Pd insertion across a C–F bond is most probably a concerted process when no electron-withdrawing group is present at the other alkyne terminus, but the mechanism changes to a stepwise one involving a zwitterionic intermediate when this terminus carries a nitro group. Although this intermediate can be located using a gas-phase computational model, a geometry optimised solvation model is necessary to properly reflect the energetic balance between the two pathways.

In the aryl series, 2-nitro substitution results in an oxygen–palladium stabilising interaction which additionally helps reduce the insertion barrier. The stepwise and concerted pathways appear more finely balanced than the nitroalkynyl system, and it is not possible to conclude from the present calculations which mechanistic pathway dominates, if indeed either does. With the fluoro η-tricarbonylchromium benzene system, the formation of an intermediate zwitterion appears sterically hindered, and only a concerted mechanism can be located at this level of theory. However, the predicted barrier for this pathway is rather higher than would be consistent with a reaction that is experimentally observed, and so we cannot exclude the possibility of other mechanistic pathways.

References

1 *Metal-catalyzed Cross-coupling Reactions*, ed. F. Diederich and P. J. Stang, Wiley-VCH, Weinheim, 1998.
2 K. Gouda, E. Hagiwara, Y. Hatanaka and T. Hiyama, *J. Org. Chem.*, 1996, **61**, 7232.
3 W. J. Scott, *J. Chem. Soc., Chem. Commun.*, 1987, 1755.
4 A. F. Littke and G. C. Fu, *Angew. Chem., Int. Ed.*, 1998, **37**, 3387.
5 D. W. Old, J. P. Wolfe and S. L. Buchwald, *J. Am. Chem. Soc.*, 1998, **120**, 9722.
6 F. Firooznia, C. Gude, K. Chan and Y. Satoh, *Tetrahedron Lett.*, 1998, **39**, 3985.
7 C. M. Zhang, J. K. Huang, M. L. Trudell and S. P. Nolan, *J. Org. Chem.*, 1999, **64**, 3804.
8 A. Zapf, A. Ehrentraut and M. Beller, *Angew. Chem., Int. Ed.*, 2000, **39**, 4153.
9 D. A. Widdowson and R. Wilhelm, *Chem. Commun.*, 1999, 2211.
10 R. Wilhelm and D. A. Widdowson, *J. Chem. Soc., Perkin Trans. 1*, 2000, 3808.
11 M. Hudlicky, *Chemistry of Organic Fluorine Compounds*, Prentice-Hall, New York, 1992.
12 J. L. Kiplinger, T. G. Richmond and C. E. Osterberg, *Chem. Rev.*, 1994, **94**, 373.
13 T. Braun, S. P. Foxon, R. N. Perutz and P. H. Walton, *Angew. Chem., Int. Ed.*, 1999, **38**, 3326.
14 T. Braun, L. Cronin, C. L. Higgitt, J. E. McGrady, R. N. Perutz and M. Reinhold, *New J. Chem.*, 2001, **25**, 19.
15 M. Ghavshou and D. A. Widdowson, *J. Chem. Soc., Perkin Trans. 1*, 1983, 3065.
16 M. F. Semmelhack, G. R. Clark, J. L. Garcia, J. J. Harrison, Y. Thebtaranonth, W. Wulff and A. Yamashita, *Tetrahedron*, 1981, **37**, 3957.
17 R. Wilhelm, Arenetricarbonylchromium(o) Complexes in Synthesis, PhD, University of London, London, 2001.
18 M. W. Schmidt, K. K. Baldridge, J. A. Boatz, S. T. Elbert, M. S. Gorgon, J. H. Jensen, S. Koseki, N. Matsunaga, K. A. Nguyen, S. J. Su, T. L. Windus, M. Dupuis and J. A. Montgomery, *J. Comput. Chem.*, 1993, **14**, 1347–1363.
19 Gaussian 98 (Revision A. 8), M. J. Frisch, G. W. Trucks, H. B. Schlegel, G. E. Scuseria, M. A. Robb, J. R. Cheeseman, V. G. Zakrzewski, J. A. Montgomery, Jr., R. E. Stratmann, J. C. Burant, S. Dapprich, J. M. Millam, A. D. Daniels, K. N. Kudin, M. C. Strain, O. Farkas, J. Tomasi, V. Barone, M. Cossi, R. Cammi, B. Mennucci, C. Pomelli, C. Adamo, S. Clifford, J. Ochterski, G. A. Petersson, P. Y. Ayala, Q. Cui, K. Morokuma, D. K. Malick, A. D. Rabuck, K. Raghavachari, J. B. Foresman, J. Cioslowski, J. V. Ortiz, A. G. Baboul, B. B. Stefanov, G. Liu, A. Liashenko, P. Piskorz, I. Komaromi, R. Gomperts, R. L. Martin, D. J. Fox, T. Keith, M. A. Al-Laham, C. Y. Peng, A. Nanayakkara, C. Gonzalez, M. Challacombe, P. M. W. Gill, B. G. Johnson, W. Chen, M. W. Wong, J. L. Andres, M. Head-Gordon, E. S. Replogle and J. A. Pople, Gaussian, Inc., Pittsburgh PA, 1998.
20 N. Godbout, D. R. Salahub, J. Andzelm and E. Wimmer, *Can. J. Chem.*, 1992, **70**, 560 basis set for palladium: N. Godbout, PhD Thesis, Dept. Chim., University of Montreal, Quebec, Canada, 1992; Basis sets were obtained from the Extensible Computational Chemistry Environment Basis Set Database, Version 11/29/01, as developed and distributed by the Molecular Science Computing Facility, Environmental and Molecular Sciences Laboratory, Pacific Northwest Laboratory, P.O. Box 999, Richland, Washington 99352, USA. See http://www.emsl.pnl.gov:2080/forms/basisform.html.
21 M. A. Carroll, S. Martin-Santamaria, V. W. Pike, H. S. Rzepa and D. A. Widdowson, *J. Chem. Soc., Perkin Trans. 2*, 1999, 2707–2714.
22 D. S. McGuinness, K. J. Cavell and B. F. Yates, *Chem. Commun.*, 2001, 355.
23 M. N. Glukhovtsev, R. D. Bach and S. Laiter, *J. Org. Chem.*, 1997, **62**, 4036.
24 C. A. Merlic, M. M. Miller, B. N. Hietbrink and K. N. Houk, *J. Am. Chem. Soc.*, 2001, **123**, 4904.
25 A. Fretzen, A. Ripa, R. Liu, G. Bernardinelli and E. P. Kundig, *Chem. Eur. J.*, 1998, **4**, 251.